

Document downloaded from:

<http://hdl.handle.net/10251/64779>

This paper must be cited as:

Molina Alcaide, SA.; García Martínez, A.; Pastor Enguídanos, JM.; Belarte Mañes, E.; Balloul, I. (2015). Operating range extension of RCCI combustion concept from low to full load in a heavy-duty engine. *Applied Energy*. 143:211-227.
doi:10.1016/j.apenergy.2015.01.035.



The final publication is available at

<http://dx.doi.org/10.1016/j.apenergy.2015.01.035>

Copyright Elsevier

Additional Information

1

2 Operating range extension of RCCI combustion concept 3 from low to full load in a heavy-duty engine

4 **S. Molina, A. García, J.M. Pastor*, E. Belarte**

5 *CMT-Motores Térmicos*

6 *Universitat Politècnica de València*

7 *Camino de Vera s/n, 46022, Valencia (Spain)*

8 *Tel. (0034) 96 387 76 50 / Fax (0034) 96 387 76 59*

9 **I. Balloul**

10 *VOLVO Group Trucks Technology*

11 *99, Route de Lyon, 69806, Saint Priest (France)*

12 *Tel. (0033) 4 72 96 89 15 / Fax (0033) 4 72 96 82 14*

13 **Abstract**

14 Fuel reactivity controlled compression ignition (RCCI) concept has arisen as a solution
15 to control premixed combustion (PCI) strategies, which avoids soot and NO_x formation
16 by promoting a lean air-fuel mixture and low temperature combustion. Thus, this study is
17 focused on investigating the effects of different engine operating variables over
18 combustion, to be able to suggest suitable strategies for extending the RCCI operation
19 from low to full load, in a HD single-cylinder research engine.

20 Different strategies are implemented at low, medium and high load, varying fuel and air
21 reactivity, by means of parametrical studies. Performance and emissions results are
22 analyzed combining engine testing with 3D-CFD modeling. Based on those results, an
23 *overlimit function* is used to select the best engine settings for each operating point.
24 Finally, engine emissions and performance results from that RCCI operation are
25 compared with conventional Diesel combustion (CDC).

26 Results suggest that double injection strategies should be used for RCCI operation from
27 low to mid load. However, from high to full load operation, single injection strategies
28 should be used, mainly to avoid excessive in-cylinder pressure gradients. In addition, it
29 is confirmed the suitability of RCCI combustion to overcome the soot-NO_x trade-off
30 characteristic of CDC, from 6 to 24 bar of BMEP, while improving fuel consumption.

31 **Keywords:**

32 Reactivity controlled compression ignition; Dual fuel combustion; emissions control;
33 engine efficiency

34
35

** Corresponding author*

36 *Email: jopasen@mot.upv.es*

37 *Phone: (0034) 96 387 76 50 (Ext: 76545) // Fax: (0034) 96 387 76 59*

39 **1. Introduction**

40 The volume of global transport could be double or even quadruple by 2050, according to
41 a new study released by the International Transport Forum [1]. Strong increases in
42 transport volumes mean strong growth of emissions from transport. In addition, estimates
43 indicate that heavy duty vehicles are the second-biggest source of emissions within the
44 transport sector, larger than both international aviation and shipping. As a consequence,
45 the world's leading manufacturers of heavy-duty trucks and engines endorsed a
46 harmonized global approach in improving energy efficiency and reducing harmful
47 emissions from commercial vehicles [2]. Accordingly, the efforts of the scientific
48 community are focused on a combination of in-cylinder reduction strategies and exhaust
49 gas after-treatment technologies, because the difficulties faced for reducing the cost of
50 after-treatment devices, highlight the potential of in-cylinder strategies to control
51 emissions.

52 On the one hand, mixing-controlled low temperature combustion (MC-LTC) has been
53 widely investigated as a combustion technology to avoid soot and NO_x engine-out
54 emissions [3]. As conventional Diesel combustion, MC-LTC strategy is based on the
55 coexistence of injection and combustion events. Thus, combustion phasing can be
56 controlled by means of the injection timing, whatever the operating conditions. To attain
57 low temperature combustion (LTC), the use of high injection pressures and downsized
58 nozzle diameters is needed (to reduce the equivalence ratio at lift-off), and a sharp
59 decrease of the in-cylinder temperature or the intake oxygen concentration ($YO_{2,IVC}$) is
60 also needed (to reduce combustion temperatures) [4]. Despite the MC-LTC ability to
61 avoid soot and NO_x emissions formation processes [5], real application in production
62 engines is compromised. The use of massive exhaust gas recirculation (EGR) to reduce
63 $YO_{2,IVC}$ implies an ISFC and therefore BSFC problem, and the use of the Miller cycle to
64 reduce compression temperature still needs further development to reduce BSFC [6].

65 On the other hand, premixed combustion (PCI) strategies use volumetric auto-ignition to
66 achieve high levels of efficiency, and combustion in lean or dilute mixtures which result
67 in combustion temperatures too low for significant NO_x formation, and air-fuel mixtures
68 (A/F) too lean for soot formation [7]. In PCI strategies, combustion timing is mainly
69 determined by chemical kinetics, so the entire history of temperature, pressure and
70 composition of the in-cylinder charge affect to ignition timing. In this sense, the main
71 challenges of PCI strategies are combustion phasing control, noise, HC and CO emissions
72 reduction, and the operation range extension [8]. In order to address those challenges,
73 mixture preparation has been investigated by improving the mixing rate of air and fuel,
74 and by extending the ignition delay. Strategies to improve the air/fuel mixing rate are
75 mainly the use of high injection pressures with small nozzle holes, to improve atomization
76 and increase the relative velocity of the fuel injected in the cylinder and the surrounding
77 air [9]; the use of high boost pressures, to increase the in-cylinder density [10]; and the
78 use of multi-pulse fuel injection, to create mixture stratification which avoids excessive
79 rates of heat release [11, 12]. Moreover, strategies to extend the ignition delay are mainly:
80 the use of EGR, to reduce $YO_{2,IVC}$ and increase in-cylinder specific heat capacity, which
81 slows down the temperature rise during compression stroke [13]; the use of variable valve
82 actuation systems, to reduce the effective compression ratio, controlling in-cylinder
83 temperature histories [14]; the use of fuel reactivity control strategies, to modify fuel auto-
84 ignition characteristics [15].

85 In this research work, the above control strategies for PCI operation are not used alone
86 because their combination is more effective, as reported in other investigations [16, 17].
87 This approach is commonly referred to as reactivity controlled compression ignition
88 (RCCI) combustion, and relies on in-cylinder fuel blending of low reactivity fuel injected
89 through the intake port, and high reactivity fuel injected directly in the cylinder. The use
90 of one injection system for each fuel allows optimizing fuel reactivity on almost a cycle
91 to cycle basis, by varying the ICFB ratio, according to changes in engine operating
92 conditions.

93 Authors' previous work on RCCI combustion was focused on basic understanding of
94 mixing and auto-ignition processes and its influence on engine-out emissions, at low load
95 operating conditions [18]. It was found that in-cylinder fuel blending generates fuel
96 reactivity stratification, which is accompanied by equivalence ratio stratification,
97 promoting a staged combustion process, which avoids high peaks of rate of heat release.

98 On the side of the technological potential of RCCI combustion concept, several
99 investigations have been carried out [19 - 22]. Using a HSDI engine to evaluate the
100 concept all over the operating range, experiments highlight promising results at part load,
101 but important issues with smoke emissions and in-cylinder maximum pressure gradients
102 at high load operation [19]. In addition, using a HD Diesel engine, experimental work
103 focused on extending the operating range of the concept resulted in high efficiency and
104 clean combustion. However, those results were obtained in a range from low to medium
105 load operation (up to 15 bar IMEP) [20, 21]. Moreover, when trying to attain higher load
106 operation, experiments from other research work [22] show that they have to be carried
107 out modifying engine hardware (reducing the compression ratio down to 12, to reach 20
108 bar BMEP). This fact leads to define the main objective of this research work.

109 **2. Objectives and methodology**

110 The investigation has been performed to increase the existing knowledge of advanced
111 combustion strategies. In particular, the main objective of this research work is to extend
112 the RCCI operating range, in a heavy duty Diesel engine. As well, the influence of
113 different engine operating variables of this combustion strategy is analyzed in terms of
114 combustion performance and engine-out emissions.

115 To find suitable RCCI operation strategies, research has been based on parametrical
116 studies of ICFB, in-cylinder thermodynamic conditions and fueling strategies, at low (≈ 6
117 bar BMEP), medium (≈ 12 bar BMEP), high (≈ 17 bar BMEP) and full load (≈ 24 bar
118 BMEP) operating conditions. The analysis has been carried out by single cylinder engine
119 testing, supported by 3D-CFD modeling, so trends followed by pollutant emissions are
120 related to local in-cylinder conditions along the combustion process.

121 In the light of the results obtained from the mentioned analysis, engine operating
122 strategies have been proposed. Those strategies have not been rigorously optimized, they
123 have been selected from the parametrical studies using an *overlimit function*. This is a
124 mathematical function that provides a simple parameter to quantify the extent to which a
125 given combustion strategy is able to simultaneously achieve all relevant constraints [23].
126 It is defined as Equation 1 shows, where F is the *overlimit function*, x_i is the value of the
127 i^{th} constrained parameter, x_i^* is the constraint of the i^{th} parameter and i is the index over
128 all of constraints. F will be zero if only the measured value is less than or equal to the
129 specified limit.

130
$$F = \sum_i \max\left(0, \frac{x_i}{x_i^*} - 1\right)$$

131 Equation 1. Overlimit function definition.

132 In this application, constrained parameters are soot and NO_x at the limitation from EURO
133 VI regulation (0.01 and 0.4 g/kWh, respectively); also BSFC, at the level of fuel
134 consumption measured from conventional Diesel combustion tests (variable depending
135 on the engine operating conditions); and the last one, a mechanical constraint (pressure
136 gradient < 22 bar/CAD), as recommended by engine manufacturer. Furthermore, if this
137 function turns out to be zero for various strategies, a new *overlimit function* with two
138 more constrained parameters is used to select the best one between them. Those
139 parameters are HC and CO emissions, at the level of EURO VI limits (0.13 and 1.5
140 g/kWh, respectively).

141 To conclude the research work, engine performance and emissions results from the
142 selected strategies at each operating condition, are critically compared with the results
143 obtained using conventional Diesel combustion (settings from commercially available
144 truck engines, to which is equivalent the SCE used in this investigation). This final
145 comparison was conducted based on experimental measurements.

146 Basic engine operation conditions are defined by 1200 rpm and constant injected fuel
147 mass, at each engine load mode. Further development, based on the results obtained from
148 this research, will be needed to extend the RCCI concept to the whole engine operation
149 map.

150 **3. Experimental setup**

151 In comparison with multi-cylinder engines, single-cylinder engines generate more
152 accurate data [24]. Accordingly, a single-cylinder engine was used in this research work.
153 The main characteristics of the engine and the test cell are described below.

154 *3.1. Single cylinder engine*

155 The engine is a single-cylinder, four-stroke, compression ignition research engine,
156 representative of commercial truck engines. Basic specifications of this engine are given
157 in Table 1.

158 The engine is equipped with a hydraulic VVA system, so all valves are independently
159 actuated by different hydraulic pistons (one per valve), which are controlled by a specific
160 electronic control unit. The main benefit of this VVA system is its high flexibility,
161 including variable timing, duration and lift for each valve. Thus, using this system, many
162 strategies can be performed in the engine (such as Miller cycle). As a counterpart, this
163 system requires an adapted cylinder head different from the conventional design
164 (although the structural changes are not extreme) and also a dedicated oil circuit in
165 addition to the standard oil lubricating system.

166 One of the specificities of the hydraulic valve actuation is its fast-motion intake and
167 exhaust valve lift profiles. Increasing the exhaust valves opening and closing speeds is
168 interesting for reducing gas energy losses by shortening the time in which the exhaust gas
169 flow evolves under sonic conditions [25]. However, this fast-motion together with the
170 very little clearance between the piston and valves, when the piston is close to top dead

171 centre (TDC), make the valve overlap at breathing TDC impossible due to direct
172 mechanical interference between the piston and the valves. This lack of valve overlap
173 slightly reduces the engine volumetric efficiency.

174 Additionally, the engine is equipped with two different injection hardware, one for each
175 different fuel used. Commercially available Diesel and gasoline 98 ON fuels were
176 selected as high and low reactivity fuels, respectively. Their main properties are listed in
177 Table 2. On the one hand, Diesel fuel was injected by means of a common-rail direct
178 injection system (Bosch CRSN 4.2), capable to perform up to five injections per cycle
179 and to amplify common-rail fuel pressure by means of a hydraulic piston directly installed
180 inside the injector. On the other hand, gasoline was injected by means of a port fuel
181 injection system, in which two injectors are placed at the intake port, as is described in
182 [18].

183 *3.2. Test cell*

184 The engine is installed in a fully instrumented test cell, with all the auxiliary facilities
185 required for its operation and control, as is illustrated in Figure 1.

186 To achieve stable intake air conditions, an externally driven screw compressor supplied
187 the required boost pressure, before passing through an air dryer. Air pressure was adjusted
188 in the intake settling chamber, while intake temperature was controlled in the intake
189 manifold, after mixing with EGR. The exhaust backpressure produced by the turbine in
190 the real engine was replicated by means of a valve placed in the exhaust system,
191 controlling the pressure in the exhaust settling chamber.

192 A low pressure EGR circuit is also installed on the engine test bench. Once solid particles
193 and liquid droplets were removed from the cooled exhaust gases, an externally driven
194 roots-type supercharger was used to increase the exhaust gas pressure over the intake
195 pressure. Then, the exact EGR rate was controlled by means of a valve between the EGR
196 settling chamber and the intake pipe, so the required exhaust gas mass flow was
197 introduced into the intake duct depending on the desired EGR rate. The temperature
198 regulation was performed upon the EGR-fresh air mixture by means of a temperature
199 sensor in the intake manifold.

200 The EGR rate was calculated using the experimental measurement of intake and exhaust
201 CO₂ concentration. The concentrations of NO_x, CO, HC, intake and exhaust CO₂, and O₂
202 were measured with specific state-of-the-art analyzers (Horiba MEXA 7100 DEGR).
203 Smoke emission was measured with a variable sampling smoke meter (AVL 415),
204 providing results directly in Filter Smoke Number units (FSN) that were transformed into
205 dry soot mass emissions by means of the correlation proposed by Christian et al. [26].

206 The in-cylinder pressure traces from a piezo-electric transducer (Kistler 6125B) were
207 recorded during 100 engine cycles, in order to compensate for dispersion in engine
208 operation. The recorded values of in-cylinder pressure were processed by means of a
209 combustion diagnosis code (CALMEC) [27, 28], which provides valuable information
210 such as the rate of heat release (RoHR) and the unburned gases temperature. The latest
211 mentioned is a basic input for the adiabatic flame temperature (T_{ad}) calculation, according
212 to the scheme proposed by Way [29].

213 To ensure the reliability of the provided results, every operation point was measured three
214 times and a reference point was controlled before every testing session, to assure tests
215 repeatability along the study.

216 **4. CFD modeling approach**

217 The computational model was built by means of CONVERGE CFD code [30]. Closed-
218 cycle computations on sector grids with periodic boundaries were carried out to improve
219 computational efficiency. In these calculations $1/9^{th}$ of the combustion chamber, due to
220 the 9-hole nozzle, is modeled. The CFD code uses a structured cartesian grid with base
221 cell size of 1.6 mm, an adaptive mesh refinement (AMR), as well as a fixed refinement
222 within the spray region. In addition, an additional volume on the cylinder head is
223 employed to match engine compression ratio. Figure 2 shows clips of the final mesh
224 configuration, at two different time steps, to illustrate the mentioned additional volume
225 and the AMR.

226 Calculations run from intake valve closing (IVC) with initial thermodynamic conditions,
227 as well as wall temperatures, estimated from experimental data by means of CALMEC
228 combustion diagnostics code.

229 The port-fuel injected gasoline is considered to be homogeneously mixed and vaporized
230 at IVC. The Diesel injection process is simulated by the standard Droplet Discrete Model
231 [31]. Spray atomization and break-up are simulated by means of the KH-RT [32] model.
232 Diesel fuel physical properties are given by the *diesel2* fuel surrogate available in
233 CONVERGE. Turbulent flow is modeled by means of the RNG k- ϵ model with wall-
234 functions [33], in order to account for wall heat transfer.

235 Concerning combustion modeling, a direct integration of detailed chemistry approach
236 was used by means of the CONVERGE code and the SAGE solver. A multi-zone model
237 from Babajimopoulos et al.[34] is used to solve the detailed chemistry in zones, i.e.,
238 groups of cells that have similar thermodynamic state, in order to speed-up chemistry
239 calculations. Cells are grouped based in two variables, temperature and equivalence ratio.
240 Calculations are performed using a 5 K bin size for temperature and 0.01 bin size for
241 equivalence ratio zones.

242 A Primary Research Fuel (PRF) (n-heptane + iso-octane) has been used as fuel surrogate.
243 This kinetic mechanism [35] is composed by 45 species and 142 reactions, including NOx
244 formation (thermal, N₂O and NO₂ pathways). Soot formation and oxidation is modeled
245 by a phenomenological two-step model which uses acetylene as soot precursor [36]

246 **5. Results and discussion**

247 In previous studies [18], the use of an in-cylinder fuel blending ratio of 25% Diesel and
248 75% gasoline (ICFB 75) and a single Diesel injection strategy placed at -24 CAD aTDC,
249 resulted in smooth and well-timed rate of heat release, at low load operation. Also
250 working at low load conditions, other researchers have attained successful results, (high
251 efficiency, low NOx and low soot emissions) from RCCI operation with double Diesel
252 injection strategies [37]. Therefore, in this research work both mentioned strategies have
253 been analyzed at different operating conditions, (combined with the sweeps of ICFB,
254 injection timing/s and fuel distribution) to be able to provide suitable engine settings for
255 extending the engine operating range of the RCCI concept from low to full load.

256 *5.1. RCCI low load operation*

257 Table 3 (a) summarizes the main operating conditions fixed and swept, following
258 parametric studies, at low load. In this case, the most important engine variables fixed
259 were speed, total fuel mass and air mass flow. Using a single injection strategy, ICFB and
260 injection timing were swept. Using a double injection strategy, the first injection event
261 (SoI1) was swept while the second injection event (SoI2) was fixed; also, keeping SoI1
262 fixed, SoI2 was varied; and then, Diesel fuel split amount between injection events was
263 also swept.

264 Figure 3 contains the main results obtained from the mentioned sweeps, in terms of
265 emissions and performance. The dashed lines mark the region of interest, according to
266 EURO VI emissions regulations and fuel consumption results (in terms of percentages
267 where negative values mean an improvement with respect to the low load neat Diesel
268 combusting case). On the left side of the mentioned figure, the results from using a single
269 direct injection strategy are included; while on the right side, are the ones from using a
270 double injection strategy. Looking to the NO_x- Δ BSFC subfigure, there is a trade-off
271 when using a single injection strategy: delaying SoI and increasing the ICFB reduces NO_x
272 but increases fuel consumption. As is shown in Figure 4, those strategies imply later
273 combustion phasing, longer combustion events and, as a consequence, lower flame
274 temperatures. Thus NO_x emissions get lowered, but BSFC is increased. However, the
275 mentioned trade-off does not appear when using a double injection strategy, where
276 advanced injection events and more fuel in the first one of them are able to reduce
277 simultaneously NO_x emissions and fuel consumption. It is mainly due to those strategies
278 are able to phase combustion slightly towards the expansion stroke, without worsening
279 the RoHR (keeping almost constant duration and the peak of heat release), as shown in
280 Figure 4. In addition, as the rest of subfigures from Figure 3 show, both injection
281 strategies are able to provide soot emissions compliant with EURO VI requirements,
282 reduced pressure gradients and ~97% of combustion efficiency.

283 Important differences have been found between using single or double injection
284 strategies. To deeply analyze that behavior, single injection at -24 CAD aTDC and double
285 injection at -60/-35 CAD aTDC, using ICFB 75, have been modeled using 3D-CFD. To
286 assure the quality of the model, their results have been validated versus experimental data,
287 and as Figure 5 shows, fair predictions in terms of combustion development have been
288 obtained. Figure 6 contains a sequence of in-cylinder equivalence ratio and temperature
289 cut planes, focused from the start to the end of combustion. The higher level of NO_x
290 emissions obtained from the single injection strategy is justified by the existence of wider
291 regions of high temperature, for longer in the cycle. In terms of soot emissions both cases
292 show low levels, however it is caused by different mechanisms, as Figure 7 depicts. Using
293 single injection strategies there appear rich regions which promote soot formation;
294 however the high temperatures existing help to their oxidation resulting in low soot
295 emissions. Using double injection strategies, the high equivalence ratio regions are
296 strongly reduced, and therefore, the low level of soot emissions is ruled by avoiding its
297 formation. The mentioned lower local equivalence ratios from double injection strategies
298 provide later combustion phasing (from TDC to the expansion stroke) that contributes to
299 increase IMEP and to improve fuel consumption.

300 Hence, at low load conditions high in-cylinder fuel blending ratios and double injection
301 strategies are more adequate for RCCI operation.

302 5.2. RCCI medium load operation

303 The main operating conditions for the study at medium load are detailed in Table 3 (b).
304 This study was developed by means of parametrical studies, keeping fixed speed, total
305 fuel mass and air mass flow. As well as fuel reactivity, ambient reactivity effects over
306 combustion performance and emissions have been analyzed, due to the increased engine
307 load. Using a single injection strategy, the ICFB and the injection timing were swept.
308 Using a double injection strategy, the ICFB, SoI1 (with fixed SoI2), SoI2 (with fixed
309 SoI1); the Diesel fuel split amount between injection events; and the effective
310 compression ratio (CR_{ef}) were swept.

311 It should be noted that, in this research, the CR_{ef} was varied by implementing an early
312 Miller cycle. This strategy is based on the reduction of the CR_{ef} , and therefore, of
313 compression temperatures, by shortening the duration of the intake event by advancing
314 the intake valves closing (IVC), as Figure 8 shows. Consequently, the intake air mass is
315 reduced; to overcome this fact, the intake pressure has been increased as advanced the
316 IVC, keeping constant the intake air mass flow along the CR_{ef} sweep.

317 Figure 9 contains the main results obtained from the mentioned sweeps, in terms of
318 emissions and performance. As in Figure 3, the region of interest is defined by EURO VI
319 emissions regulation, neat Diesel fuel consumption at medium load and the limit of
320 maximum pressure gradient.

321 As is shown in the left hand subfigures from Figure 9, using single Diesel injection
322 strategies, a trade-off appears between NO_x and fuel consumption, as in low load
323 operation (the injection timing delay and the ICFB lowering reduces NO_x emissions but
324 increases fuel consumption). Moreover, an additional trade-off appears between soot and
325 NO_x emissions due to the worsening of combustion efficiency promoted by the injection
326 timing delay and the longer Diesel injection rates from lower ICFB. By contrast, the use
327 of double Diesel injection strategies is able to attain the NO_x- Δ BSFC simultaneous
328 reduction, as is shown in the right hand subfigures from Figure 9. Nevertheless, it should
329 be remarked that an advanced double Diesel injection strategy is not enough to attain the
330 region of interest, because of the early phasing of combustion, which results in high NO_x
331 emissions and fuel consumption. The last mentioned subfigures show that the strategies
332 which shift combustion towards TDC and the expansion stroke are: the ICFB lowering,
333 the advance of SoI1, the delay of SoI2, the use of fewer amount of fuel into the first
334 injection event and the lowering of the CR_{ef} . Those strategies also provide soot emissions
335 compliant with EURO VI requirements, reduced pressure gradients and combustion
336 efficiency between 97 and 98 %.

337 The most representative extremes from the mentioned strategies ($[CR_{ef} 14, SoI1 -60, SoI2$
338 -10 CAD aTDC]; $[CR_{ef} 11, SoI1 -60, SoI2 -40$ CAD aTDC]) have been compared with
339 their baseline case ($[CR_{ef} 14, SoI1 -60, SoI2 -40$ CAD aTDC]), using 3D-CFD modeling.
340 Figure 10 shows a good agreement on ignition delay though over-predicted peaks of
341 RoHR between modeling and experimental results. The cause of this over-prediction may
342 be due to chemical mechanism validity range, since higher pressure and temperature are
343 found when increasing load. Also the lack of any turbulent-chemistry interaction model
344 may also contribute to this result [38]. Nevertheless, predicted in-cylinder pressure and
345 RoHR traces show the ability to modify combustion phasing from the delay of the SoI2
346 and the reduction of the CR_{ef} .

347 To further analyze this behavior, Figures 11 and 12 contain sequences of in-cylinder
348 equivalence ratio and temperature cut planes, between the start and the end of combustion.
349 The first one compares the cases with the same CR_{ef} , and shows that the later SoI2 triggers
350 the onset of combustion. Thus, it provides a longer ignition delay which implies the later
351 appearance of high temperature zones into the combustion chamber (closer to TDC,
352 instead of earlier during the compression stroke). Therefore lower in-cylinder maximum
353 temperatures are attained. On the other hand, the second injection event creates a high
354 reactivity region, under-stratified, which promotes a faster RoHR, placed before TDC, at
355 these operating conditions. Figure 12 compares the cases with the same fueling strategy
356 and different CR_{ef} , and shows that both result in very similar equivalence ratio
357 distributions. However, their main difference is when in-cylinder temperatures
358 distributions get similar (9 CAD after for the lower CR_{ef} case), as Figure 10 shows. The
359 CR_{ef} lowering reduces compression temperatures, enabling much longer ignition delay
360 (CA25 takes place around -10 CAD aTDC for the higher CR_{ef} case, while around -4 for
361 the lower CR_{ef}). As main consequence, combustion tends to take place during the
362 expansion stroke, improving the level of NOx emissions and fuel consumption.

363 According to this analysis, high ICFB and double Diesel injection strategies, coupled with
364 lowered in-cylinder thermodynamic conditions, provide the best results for medium load
365 RCCI operation.

366 *5.3. RCCI high load operation*

367 As in previous subsections, Table 3 contains the main operating conditions, particularized
368 for the study at high load in column (c). In this study, as well as speed, total fuel mass
369 and air mass flow, $CR_{ef} = 11$ was also fixed (CR_{ef} was reduced on the light of the results
370 from the medium load analysis and considering the increase on engine load). Using a
371 double injection strategy, SoI1 was swept while SoI2 was fixed; and SoI2 was varied with
372 a fixed SoI1. In both sweeps the fuel split ratio was set at 50 / 50 between injection events.
373 Then, using a single injection strategy, the ICFB and the injection timing were also swept.

374 Figure 13 contains the emissions and performance results obtained from the mentioned
375 sweeps, and the region of interest marked with dashed lines. Right hand subfigures show
376 the results from using double Diesel injection strategies, while the left hand ones show
377 the results from using single Diesel injection strategies. Despite the lowered in-cylinder
378 thermodynamic conditions from the reduced CR_{ef} , when using a double injection strategy,
379 the main challenge is the extremely high in-cylinder maximum pressure gradient. Even
380 delaying both injection timings, pressure gradients still too high and combustion starts
381 before the SoI2, burning the second injection event in a high temperature and fuel rich
382 region, which promotes high soot formation. Regarding NOx emissions, mainly the SoI2
383 delay is able to reduce them, but remaining far away from the region of interest. Then, a
384 single injection strategy was tested trying to improve high load engine operation. As
385 found at lower operating loads, the NOx- Δ BSFC subfigure on the left side of Figure 13
386 shows a trade-off when lowering ICFB and delaying injection timing: the lower NOx, the
387 higher fuel consumption. In terms of soot emissions, they remain below the EURO VI
388 limit, mainly due to high load operation implies enhanced combustion efficiency and
389 improved oxidation processes. Aside from those findings, the most important result is that
390 single injection strategies, placed close to TDC, attain adequate in-cylinder maximum
391 pressure gradients, enabling RCCI operation at high load.

392 The cases selected to perform the analysis of in-cylinder local conditions are a single
393 injection strategy (-6 CAD aTDC) and a double injection strategy (-40/-10 CAD aTDC),
394 both with ICFB 70 and CR_{ef} 11. Figure 14 shows a good agreement between experimental
395 and modeling results despite of the overpredicted peak of RoHR, as found under medium
396 load conditions. Moreover, this figure highlights the great difference in terms of
397 combustion phasing between both strategies. Figure 15 contains a sequence of in-cylinder
398 temperature and equivalence ratio cut planes, starting just after the SoC of the double
399 Diesel injection case and finishing before the EoC of the single Diesel injection case.
400 There is shown that, when using the double injection strategy, the first injection ignites
401 before the second one and high temperatures are attained much earlier than in the single
402 injection case. That is the main reason of the slight influence of SoI2 over combustion
403 phasing, as Figure 16 reports. Following with the analysis from Figure 15, using a double
404 injection strategy, as the second injection burns, high temperature regions are extended
405 to a wider region of the combustion chamber. It is coherent with the high levels of NOx
406 and the low levels of soot emissions measured. By contrast, when using a single injection
407 strategy, combustion is triggered by the Diesel injection and progresses through the
408 Diesel spray (high equivalence ratio and reactivity zones), keeping high temperature
409 regions there. Thus, at these conditions, the single Diesel injection strategy is able to
410 control RCCI combustion, as is shown in Figure 16.

411 Hence, at high load conditions single injection strategies provide better results for RCCI
412 operation, mainly due to its capability to keep controlled in-cylinder maximum pressure
413 gradients.

414 5.4. RCCI full range operation

415 In this subsection the RCCI operation is experimentally demonstrated over a range of
416 loads from 25% (\approx 6 bar BMEP) up to 100% (\approx 24 bar BMEP).

417 Results presented here have been selected by using the *overlimit function* as detailed in
418 section 2, from a different number of experiments. It means that the engine operating
419 variables are not fixed over the load sweep. Moreover, these have not been rigorously
420 optimized, so it is expected that different combinations of injection parameters, EGR
421 levels and ICFB may yield similar results.

422 As has been proved in the previous subsection, in-cylinder maximum pressure gradients
423 and combustion phasing become a concern when increasing engine load. Thus, to extend
424 the operation range with safe combustion performance and adequate combustion phasing,
425 in-cylinder fuel blending ratio, injection timing/s, injection pressure and fuel distribution
426 between injection events, as well as engine effective compression ratio have been tuned,
427 providing suitable RCCI operating strategies all over the load range. Figure 17
428 summarizes the main settings adopted for the variables tuned, represented versus BMEP,
429 as load indicator.

430 Best results at low load operation, 6 bar BMEP, are attained by means of ICFB 75 and a
431 double injection strategy, with 60% of the Diesel fuel mass injected into the pilot event
432 at -60 CAD aTDC and the rest at -15 CAD aTDC. At medium load operation, 12 bar
433 BMEP, the best results are provided by ICFB 80 and early double injection strategy (-
434 60/-40 CAD aTDC), with the same amount of Diesel fuel in each event. It should be
435 remarked that, this combustion strategy requires lowered CR_{ef} to maintain adequate
436 combustion phasing and safe pressure gradients. Thus, up to medium load, RCCI

437 combustion results EURO VI compliant in terms of NO_x and soot emissions,
438 simultaneously.

439 As has been detailed before, high load operation using double Diesel injection strategies
440 provides too high pressure gradients, which make this strategy not suitable for this
441 operating condition, (at least keeping this hardware configuration). Accordingly, at 17
442 bar BMEP, the best results were attained with ICFB 60 and a single Diesel injection, close
443 to TDC (-6 CAD aTDC). Further engine load increase, up to 24 bar BMEP (full load),
444 needs a close to TDC single Diesel injection and also a reduction of the premixed gasoline
445 ratio to keep autoignition under control. Hence, full load best results were obtained using
446 ICFB 40 and single Diesel injection placed -8 CAD aTDC. The main drawback from the
447 strategies used at high load is the increase in terms of NO_x emissions, due to the high
448 flame temperatures resulting from the coexistence of Diesel injection and combustion
449 events, as the plot of maximum adiabatic temperature of Figure 18 shows.

450 *5.5. RCCI comparison with CDC*

451 In the previous subsection suitable RCCI operating strategies have been suggested to be
452 used in the entire engine load range. Then, to complete the study, performance and
453 engine-out emissions from those engine operating strategies are directly compared with
454 conventional Diesel combustion (CDC), at the same speed and load conditions. CDC
455 settings were provided from the equivalent commercial truck engine (which was designed
456 to operate with EGR and SCR), by the engine manufacturer supporting this research work.
457 Note that, to be a fair comparison, CDC experiments were conducted with the same SCE,
458 detailed in section 3. The key operation parameters for the comparison are included in
459 Figure 17. Performance and emissions results from RCCI and CDC are compared in
460 Figure 18.

461 Looking to the last mentioned figure, the main drawbacks from RCCI combustion
462 strategy are: higher in-cylinder maximum pressure gradients at high load operation and
463 lower combustion efficiency all over the load range. Regarding pressure gradients, the
464 much more premixed conditions from RCCI combustion strategy, implies higher pressure
465 gradients when compared with the mixing-controlled strategy used in CDC. Concerning
466 combustion efficiency challenge, it is mainly related with the incomplete combustion of
467 low reactivity fuel existing at cold regions. On the other hand, Figure 18 highlights as
468 main benefits from RCCI combustion lower soot and NO_x emissions, and also
469 competitive fuel consumption whatever the load conditions. Looking at soot results,
470 RCCI is much better at full load operation, because this strategy promotes lean
471 equivalence ratios that avoid soot formation, while mixing-controlled combustion
472 (specially with medium injection pressures) results in a large soot formation rate. On the
473 concern of NO_x emissions, the lower adiabatic flame temperatures achieved by the RCCI
474 mode avoid NO_x formation processes, especially at medium-low load operation, where a
475 double injection strategy is used. Regarding fuel consumption, RCCI mode only shows
476 worse results than CDC at the 17 bar operating point. It is mainly due to the higher
477 pumping work from the p-V low pressure loop that Miller cycle implies [6], and the
478 higher RCCI global equivalence ratio (0.78 vs. 0.57) which deal with a lower polytropic
479 index, and therefore worse fuel conversion efficiency. This issue could be solved by
480 engine optimization methodology; however this is not the aim of this research and
481 remains for further work on this topic. Moreover, despite both combustion strategies
482 attain correctly phased CA₅₀ whatever the engine load, RCCI combustion event is much

483 shorter, which makes the better thermal efficiency compensate the worse combustion
484 efficiency, resulting in similar or better BSFC levels than CDC.

485 **6. Conclusions**

486 Present study focuses on extending the RCCI operating range from low to full load, using
487 a heavy-duty single-cylinder research engine to analyze different engine variables, which
488 lead to the definition of suitable operating strategies.

489 The research is based on different sets of parametric studies. However, multi-dimensional
490 CFD simulations resulted essential to gain an insight of in-cylinder local conditions.

491 Engine performance and emissions have been analyzed at low, medium and high load
492 conditions, by combining single cylinder engine testing with 3D-CFD modeling. This
493 study provided the following conclusions:

- 494 • At low load conditions high ICFB and double direct injection strategies provide
495 better results than single injection strategies. Mainly due to the longer ignition
496 delays and the latter combustion phasing from the earlier injection timings, which
497 help to reduce in-cylinder temperatures during combustion and to lower zones
498 with rich equivalence ratios, reducing simultaneously soot and NO_x emissions to
499 almost zero.
- 500 • At mid load conditions, high ICFB and double direct injection strategies need to
501 be coupled with lowered in-cylinder thermodynamic conditions to keep
502 autoignition under control. This fact implies low maximum adiabatic flame
503 temperatures that avoid NO_x formation mechanisms, and lean equivalence ratios
504 that avoid soot inception.
- 505 • At high load conditions, single direct injection strategies are able to trigger
506 combustion by means of the injection timing. It permits to attain an adequate
507 combustion phasing and to control in-cylinder maximum pressure gradients, from
508 the two-staged heat release.

509 Then, using an *overlimit function* suitable settings for RCCI operation from low to full
510 load are provided. In addition, their performance and emissions results have been
511 compared with CDC, at the same speed and load conditions.

- 512 • From the high ICFB and double direct injection strategy used at low load, when
513 increasing to medium load, RCCI operation needs to lower the effective
514 compression ratio. Further increase to high load, also needs the use of single direct
515 injection strategies, close to TDC. And to reach full load, is also necessary the
516 lowering of the ICFB (reducing the amount of premixed gasoline).
- 517 • Comparing the results between RCCI and CDC, the main drawback from RCCI
518 is its lower combustion efficiency (especially at low load) and its higher in-
519 cylinder maximum pressure gradients (from medium to full load operation). By
520 contrast, soot and NO_x emissions levels are simultaneously better than CDC,
521 whatever the load conditions. In addition, fuel consumption results are also
522 improved at every operating condition, except around 17.5 bar BMEP where still
523 competitive but 1% higher.

524 From this investigation, suitable settings have been provided to extend the RCCI
525 operating range from low to full load. Moreover, it has been demonstrated how the RCCI
526 combustion concept is capable to solve the soot-NO_x trade-off characteristic of CDC, all

Paper draft:

Operating range extension of RCCI combustion concept from low to full load in a heavy-duty engine

527 over the engine load range. However, the main challenge for RCCI application in
528 production engines is the lowering of NO_x emissions from high-to-full load operation.
529 Thus, further research on this topic is still needed to improve the reactivity stratification
530 at high load operating conditions, to control combustion progression and to reduce NO_x
531 emissions level, avoiding the need of SCR technologies.

532 **7. Acknowledgments**

533 The authors would like to recognize the technical support from VOLVO Group Trucks
534 Technology. In addition, the authors would also like to thank Gabriel Alcantarilla for the
535 management of the facility and his assistance in data acquisition.

536

537

538

539

540 **References**

- 541 1. OECD/International Transport Forum (2013), ITF Transport Outlook 2013: Funding Transport,
542 OECD Publishing/ITF. Doi:[10.1787/9789282103937-en](https://doi.org/10.1787/9789282103937-en).
- 543 2. Advanced internal combustion engines and fuels importance for European road transport research and
544 horizon 2020. EARPA position papers. June 2012.
- 545 3. Zamboni G, Capobianco M. Experimental study on the effects of HP and LP EGR in an automotive
546 turbocharged diesel engine. Applied Energy 2012;94:117-28, doi:10.1016/j.apenergy.2012.01.046.
- 547 4. Pickett LM, Siebers DL, Non-sooting, low flame temperature mixing-controlled DI Diesel
548 combustion. SAE paper 2004-01-1399; 2004.
- 549 5. Benajes J, Molina S, Novella R, Amorim R. Study on low temperature combustion for light-duty
550 Diesel engines. Energy and Fuels 2010;24:355-64.
- 551 6. Benajes J, Molina S, Novella R, Belarte E. Evaluation of massive exhaust gas recirculation and Miller
552 cycle strategies for mixing-controlled low temperature combustion in a heavy duty diesel engine.
553 Energy 2014;71:355-66, doi:10.1016/2014.04.083.
- 554 7. Gan S, Ng HK, Pang KM. Homogeneous Charge Compression Ignition (HCCI) combustion:
555 Implementation and effects on pollutants in direct injection diesel engines. Applied Energy
556 2011;88:559-67.
- 557 8. Yao M, Zheng Z, Liu H. Progress and recent trends in homogeneous charge compression ignition
558 (HCCI) engines. Progress in Energy and Combustion Science 2009;35:398-37.
- 559 9. Dodge LG, Simescu S, Neely GD, Maymar MJ, Dickey DW. Effect of Small Holes and High Injection
560 Pressures on Diesel Engine Combustion. SAE technical paper 2002-01-0494;2002, doi:10.4271/2002-
561 01-0494.
- 562 10. Benajes J, Novella R, García A, Arthozoul S. The role of in-cylinder gas density and oxygen
563 concentration on late spray mixing and soot oxidation processes. Energy 2011;36:1599-11.
- 564 11. Wada Y, Senda J. Demonstrating the Potential of Mixture Distribution Control for Controlled
565 Combustion and Emissions Reduction in Premixed Charge Compression Ignition Engines. SAE
566 technical paper 2009-01-0498;2009, doi:10.4271/2009-01-0498.
- 567 12. Torregrosa AJ, Broatch A, García A, Mónico LF. Sensitivity of combustion noise and NOx and soot
568 emissions to pilot injection in PCCI Diesel engines. Applied Energy 2013;104:149-57.
- 569 13. Millo F, Giacominetto PF, Bernardi MG. Analysis of different exhaust gas recirculation architectures
570 for passenger car Diesel engines. Applied Energy 2012;98:79-91.
- 571 14. Benajes J, Molina S, Martín J, Novella R. Effect of advancing the closing angle of the intake valves
572 on diffusion-controlled combustion in a HD diesel engine. Applied Thermal Engineering
573 2009;29:1947-54.
- 574 15. Han X, Zheng M, Wang J. Fuel suitability for low temperature combustion in compression ignition
575 engines. Fuel 2013;109:336-49.
- 576 16. Inagaki K, Fuyuto T, Nishikawa K, Nakakita K, Sakata I. Dual-Fuel PCI Combustion Controlled by
577 In-Cylinder Stratification of Ignitability. SAE technical paper 2006-01-0028;2006, doi:10.4271/2006-
578 01-0028.
- 579 17. Kokjohn SL, Hanson RM, Splitter DA, Reitz R.D. Experiments and Modeling of Dual-Fuel HCCI
580 and PCCI Combustion Using In-Cylinder Fuel Blending. SAE technical paper, 2009-01-2647; 2009,
581 doi: 10.4271/2009-01-2647.
- 582 18. Benajes J, Molina S, García A, Belarte E, Vanvolsem M. An investigation on RCCI combustion in a
583 heavy duty diesel engine using in-cylinder blending of diesel and gasoline. Applied Thermal
584 Engineering 2014;63:66-76.

- 585 19. Duffour F, Ternel C, Pagot, A. IFP Energies Nouvelles Approach for Dual Fuel Diesel-Gasoline
586 Engines. SAE technical paper 2011-24-0065;2011, doi:10.4271/2011-24-0065.
- 587 20. Kokjohn SL, Hanson RM, Splitter DA, Reitz RD. Fuel reactivity controlled compression ignition
588 (RCCI): A pathway to controlled high-efficiency clean combustion. International Journal of Engine
589 Research 2011;12:209-26.
- 590 21. Ma S, Zheng Z, Liu H, Zhang Q, Yao M. Experimental investigation of the effects of diesel injection
591 strategy on gasoline/diesel dual-fuel combustion. Applied Energy 2013;109: 202-12.
- 592 22. Splitter D, Wissink M, Hendricks TL, Ghandhi JB, Reitz R. Comparison of RCCI, HCCI, and CDC
593 Operation from Low to Full Load. THIESEL 2012 Conference.
- 594 23. Cheng AS, Upatnieks A, Mueller CJ. Investigation of fuel effects on dilute, mixing-controlled
595 combustion in an optical direct-injection diesel engine. Energy and Fuels 2007; 21(6):3750–64.
- 596 24. Benajes J, López JJ, Novella R, García A. Advanced Methodology for Improving Testing Efficiency
597 in a Single-Cylinder Research Diesel Engine. Experimental Techniques 2008;32:41-47.
- 598 25. Benajes J, Serrano JR, Dolz V, Novella R. Analysis of an extremely fast valve opening camless system
599 to improve transient performance in a turbocharged high speed direct injection diesel engine.
600 International Journal of Vehicle Design 2009;49:192-13.
- 601 26. Christian R, Knopf F, Jasmek A, Schindler W. A New Method for the Filter Smoke Number
602 Measurement with Improved Sensitivity. MTZ Motortechnische Zeitschrift 1993;54:16-22.
- 603 27. Lapuerta M, Armas O, Hernández JJ. Diagnostic of D.I. Diesel Combustion from In-Cylinder Pressure
604 Signal by Estimation of Mean Thermodynamic Properties of the Gas. Applied Thermal Engineering,
605 1999;19:513–29.
- 606 28. Payri F, Molina S, Martín J, Armas O. Influence of measurement errors and estimated parameters on
607 combustion diagnosis. Applied Thermal Engineering 2006;26:226–36.
- 608 29. Way RJB. Methods for Determination of Composition and Thermodynamic Properties of Combustion
609 Products for Internal Combustion Engine Calculations. Proceedings of the Institution of Mechanical
610 Engineers 1976;190(60):686-97.
- 611 30. Senecal PK, Richards KJ, Pomraning E, Yang T, Dai MZ, McDavid RM, Patterson MA, Hou S,
612 Shethaji T. A New Parallel Cut-Cel lCartesian CFD Code for Rapid Grid Generation Applied to In-
613 Cylinder Diesel Engine Simulations. SAE technical paper 2007-01-0159;2007, doi:10.4271/2007-01-
614 0159.
- 615 31. Dukowicz J. A particle fluid numerical model for liquid sprays. Journal of Computational. Physics
616 1980;2:111–566.
- 617 32. Beale J, Reitz RD. Modeling spray atomization with the Kelvin–Helmholtz/Rayleigh–Taylor hybrid
618 model. Atomization and Sprays 1999;9(6):623–50.
- 619 33. Han Z, Reitz RD. A Temperature Wall Function Formulation for Variable Density Turbulence Flow
620 with Application to Engine Convective Heat Transfer Modeling. International Journal Heat and Mass
621 Transfer 1997;40.
- 622 34. Babajimopoulos A, Assanis DN, Flowers DL, Aceves SM, Hessel RP. A fully coupled computational
623 fluid dynamics and multi-zone model with detailed chemical kinetics for the simulation of premixed
624 charge compression ignition engines. International Journal of Engine Research 2005;6.
- 625 35. Ra Y, Reitz RD. A reduced chemical kinetic model for IC engine combustion simulations with
626 primary reference fuels. Combustion and Flame 2008;155.
- 627 36. Kong SC, Sun Y, Reitz RD. Modeling Diesel Spray Flame Lift-off, Sooting Tendency, and NOx
628 Emissions Using Detailed Chemistry with Phenomenological Soot Model. ASME Journal of Gas
629 Turbines and Power 2007;129:245-51.

Paper draft:

Operating range extension of RCCI combustion concept from low to full load in a heavy-duty engine

- 630 37. Hanson RM, Kokjohn SL, Splitter DA, Reitz RD. Low load investigation of reactivity controlled
631 compression ignition (RCCI) combustion in a heavy-duty engine. SAE technical paper 2011-01-
632 0361;2011.
- 633 38. Haworth DC. Progress in probability density function methods for turbulent reacting flows. Progress
634 in Energy and Combustion Science 2010;26:168–59.
- 635
- 636

637 **Nomenclature**

AMR	Adaptive Mesh Refinement
aTDC	After Top Dead Centre
A/F	Air – Fuel ratio (mass)
BMEP	Brake Mean Effective Pressure
BSFC	Brake Specific Fuel Consumption
CAD	Crank angle degree
CA25	Angle when 25% of the fuel is burnt
CA50	Angle when 50% of the fuel is burnt
CDC	Conventional Diesel Combustion
CO	Carbon monoxide
Comb. eff	Combustion efficiency
CO₂	Carbon dioxide
CR	Compression ratio
CR_{ef}	Effective compression ratio
dP/da	Pressure Gradient
EGR	Exhaust Gas Recirculation
EOC	End of Combustion
FSN	Filter Smoke Number
HC	Unburned Hydrocarbon
HD	Heavy Duty
HSDI	High Speed Direct Injection
ICFB	In-Cylinder Fuel Blending
Ign. delay	Ignition Delay
IMEP	Indicated Mean Effective Pressure
IP	Injection Pressure
ISFC	Indicated specific fuel consumption
IVC	Intake Valve Closing (angle)
LTC	Low Temperature Combustion
MC-LTC	Mixing-Controlled low temperature combustion
NO_x	Nitrogen Oxides
ON	Octane Number
O₂	Oxygen
P	Pressure
PCI	Premixed Compression Ignition
P_{int}	Intake Pressure
PRF	Primary Reference Fuel
RCCI	Reactivity Controlled Compression Ignition
RoHR	Rate of Heat Release
SCE	Single Cylinder Engine
SoC	Start of Combustion
SoI	Start of Injection
T	Temperature
T_{ad}	Adiabatic flame temperature
T_{int}	Intake temperature
TDC	Top Dead Centre
VVA	Variable Valve Actuation
YO_{2,IVC}	Oxygen concentration in the cylinder at the intake valves closing
3D-CFD	Tri-dimensional Computational Fluid Dynamics
φ	Equivalence ratio

639 **List of Figures**

1. Complete test cell schema.	19
2. Different grid refinements by CONVERGE adaptive mesh refinement.	20
3. Experimental results from the different variables swept at low load operation, using single Diesel injection (left) and double Diesel injection (right).	21
4. RoHR experimental results, from single SoI and SoI2 sweeps, at ICFB 75 and low load operation.	22
5. RoHR, in-cylinder mean pressure and temperature comparison between modeling and experimental results, for single and double injection strategies, at ICFB 75 and low load operation.	23
6. Calculated temperature and equivalence ratio cut planes for low load, single Diesel injection and double Diesel injection.	24
7. Comparison between modeling and experimental results in terms of fuel specific soot emissions, for single and double injection strategies, at ICFB 75 and low load operation.	25
8. Valves strategy employed in realizing the Miller cycle.	26
9. Experimental results from the different variables swept at medium load operation, using single Diesel injection (left) and double Diesel injection (right).	27
10. RoHR, in-cylinder mean pressure and temperature comparison between modeling and experimental results, for early SoI2 & CRef 14, late SoI2 & CRef 14 and early SoI2 & CRef 11, at ICFB 80 and medium load operation.	28
11. Calculated temperature and equivalence ratio cut planes for medium load, double injection strategies, with early SoI2 (left) and close to TDC SoI2 (right).	29
12. Calculated temperature and equivalence ratio cut planes for medium load, double injection strategies, with CRef 14 (left) and CRef 11 (right).	30
13. Experimental results from the different variables swept at high load operation, using double Diesel injection (left) and single Diesel injection (right).	31
14. RoHR, in-cylinder mean pressure and temperature comparison between modeling and experimental results, for single and double injection strategies, at ICFB 70 and high load operation.	32
15. Calculated temperature and equivalence ratio cut planes for high load, double Diesel injection (left) and single Diesel injection (right).	33
16. RoHR experimental results, from single SoI and SoI2 sweeps, at ICFB 70 and high load operation.	34
17. Best RCCI settings, selected for full range operation, and CDC settings provided by the engine manufacturer for analogue operating conditions.	35

18. Experimental results from full range RCCI and CDC operation, in terms of performance and emissions.

640

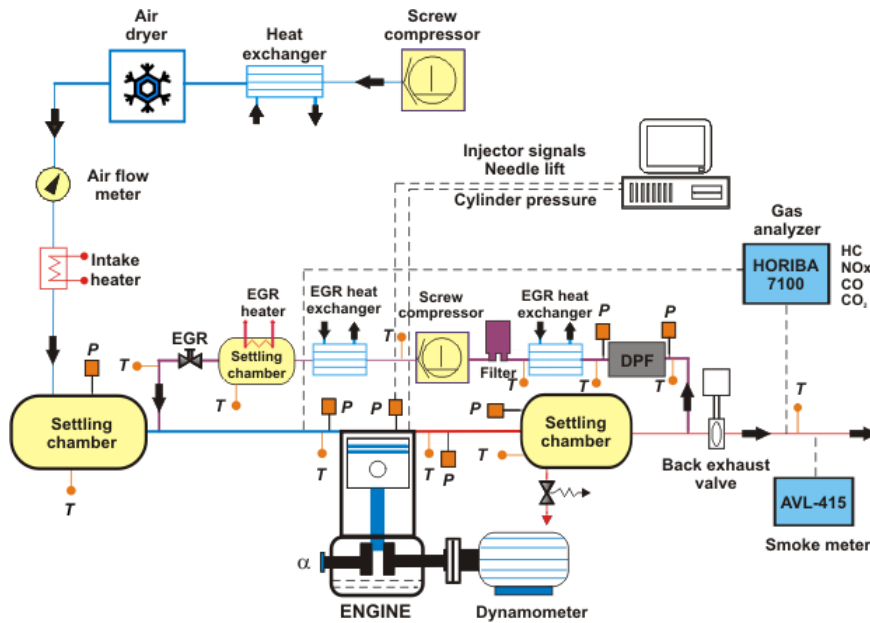
641

642

643

644

645



646

647

Figure 1: Complete test cell schema.

648

649

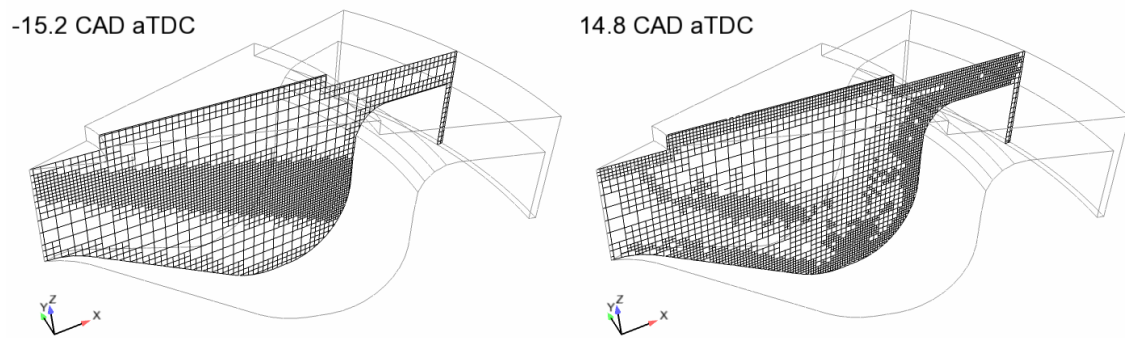
650

651

652

653

654



Computational grid at -15.2 CAD aTDC Computational grid at +14.8 CAD aTDC

655

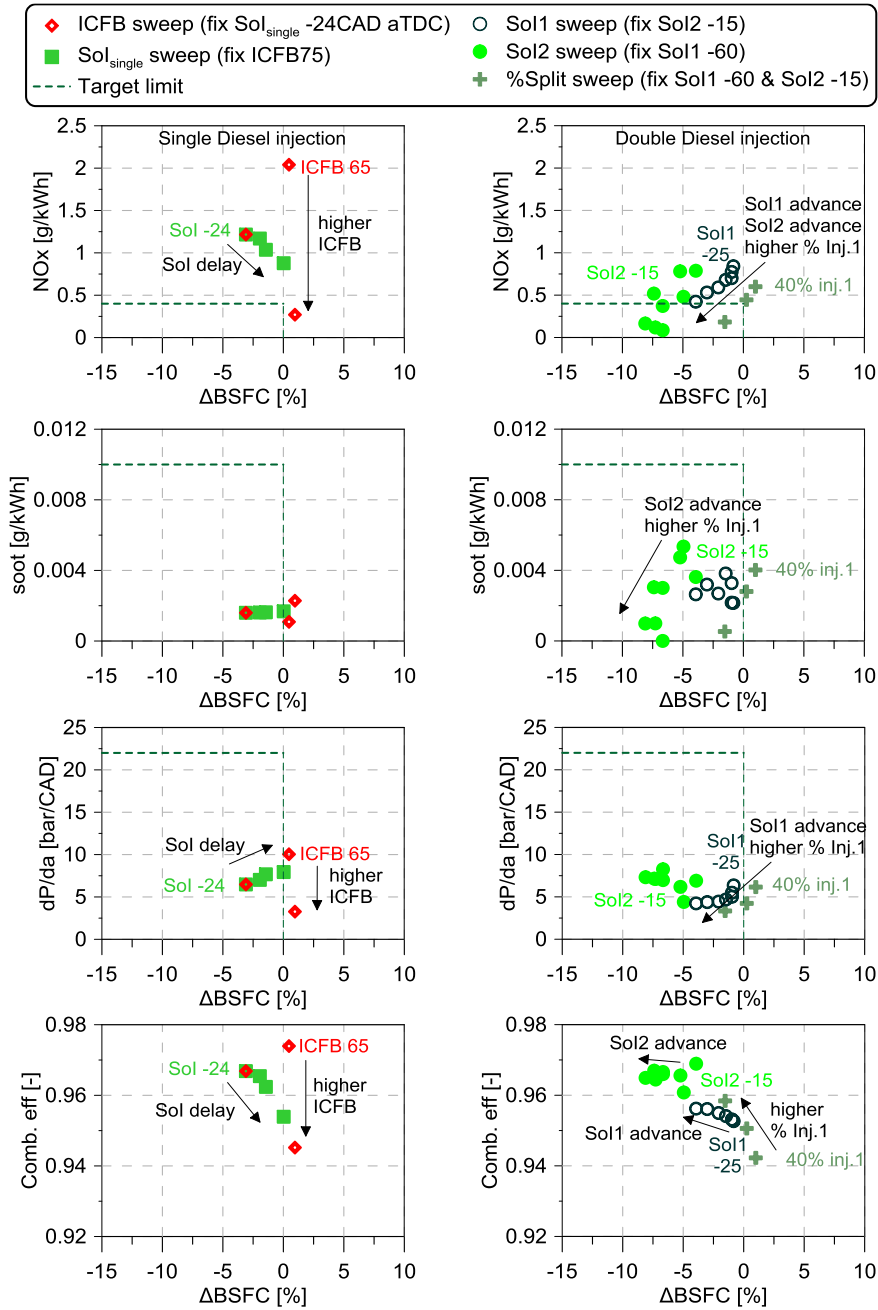
Figure 2: Different grid refinements by CONVERGE adaptive mesh refinement.

656

657

658

659



660

661 Figure 3. Experimental results from the different variables swept at low load operation,

662

using single Diesel injection (left) and double Diesel injection (right).

663

664

665

666

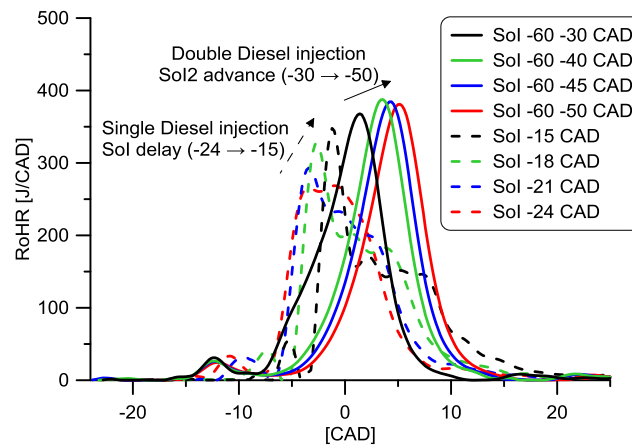
667

668

669

670

671



672

673 Figure 4. RoHR experimental results, from single SoI and SoI2 sweeps, at ICFB 75 and

674

low load operation.

675

676

677

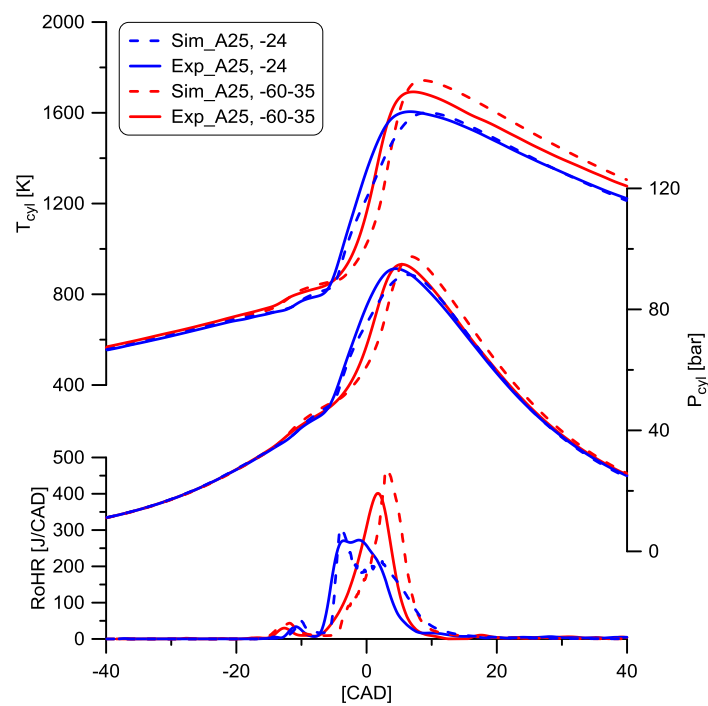
678

679

680

681

682



683

684

685

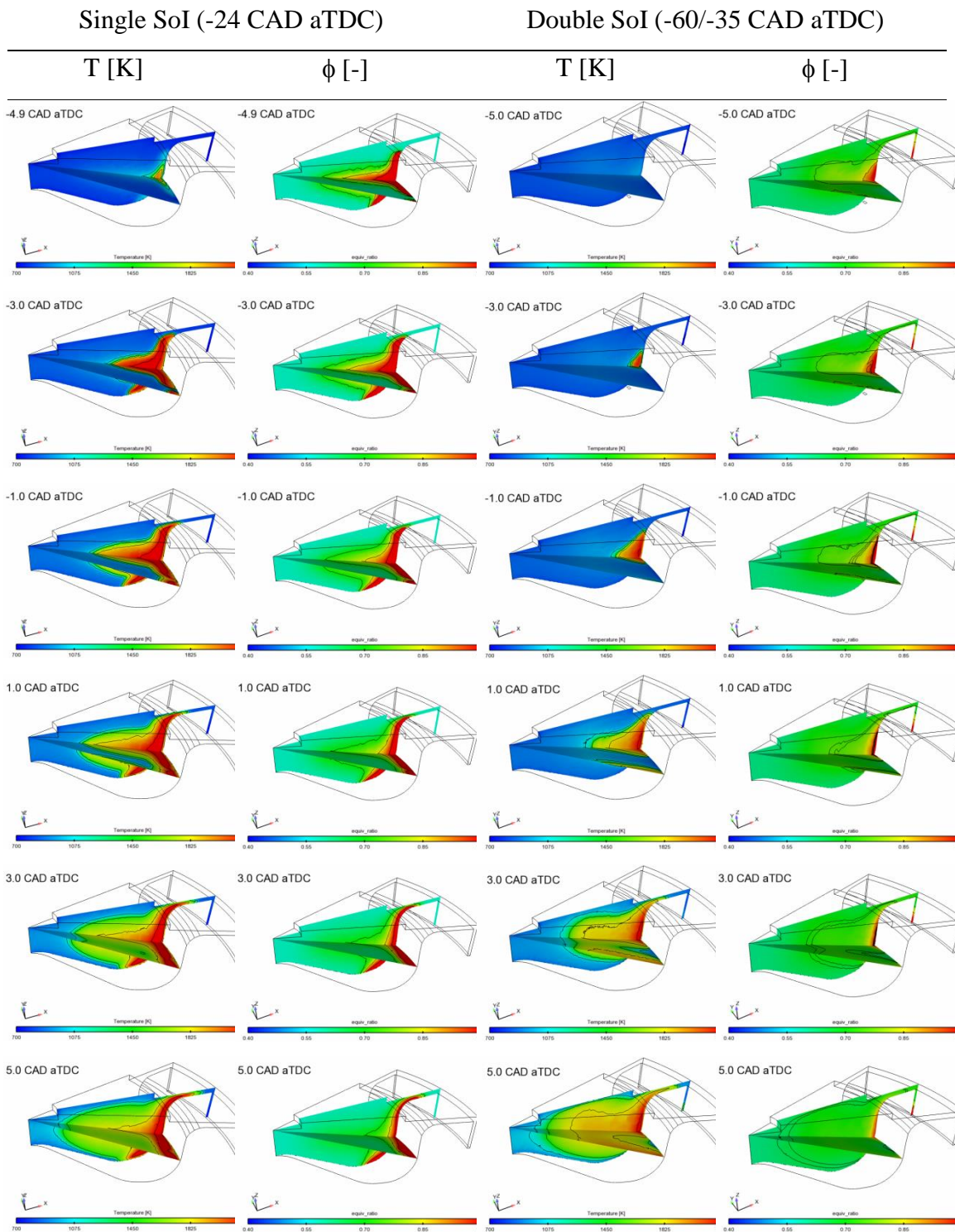
686

Figure 5. RoHR, in-cylinder mean pressure and temperature comparison between modeling and experimental results, for single and double injection strategies, at ICFB 75 and low load operation.

687

688

689



690 Figure 6. Calculated temperature and equivalence ratio cut planes for low load, single
 691 Diesel injection and double Diesel injection.
 692

693

694

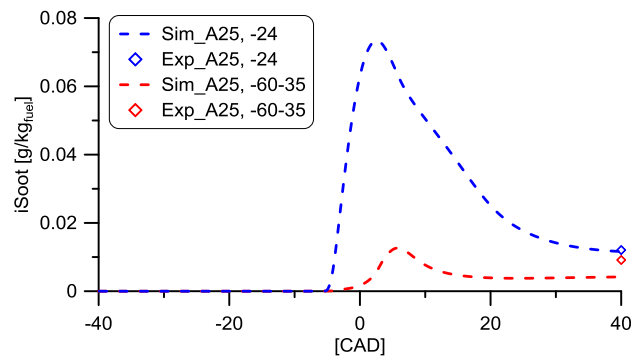
695

696

697

698

699



700

701 Figure 7. Comparison between modeling and experimental results in terms of fuel
702 specific soot emissions, for single and double injection strategies, at ICFB 75 and low
703 load operation.

704

705

706

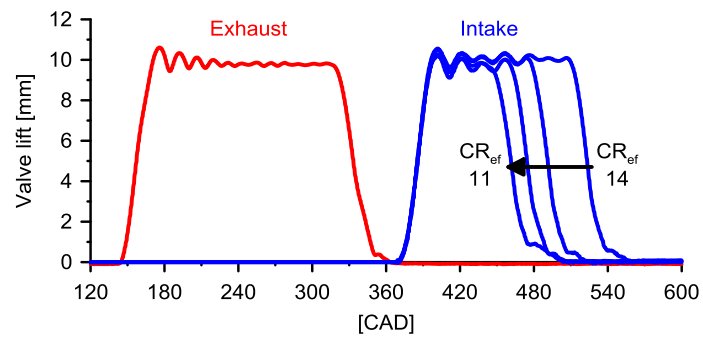
707

708

709

710

711



712

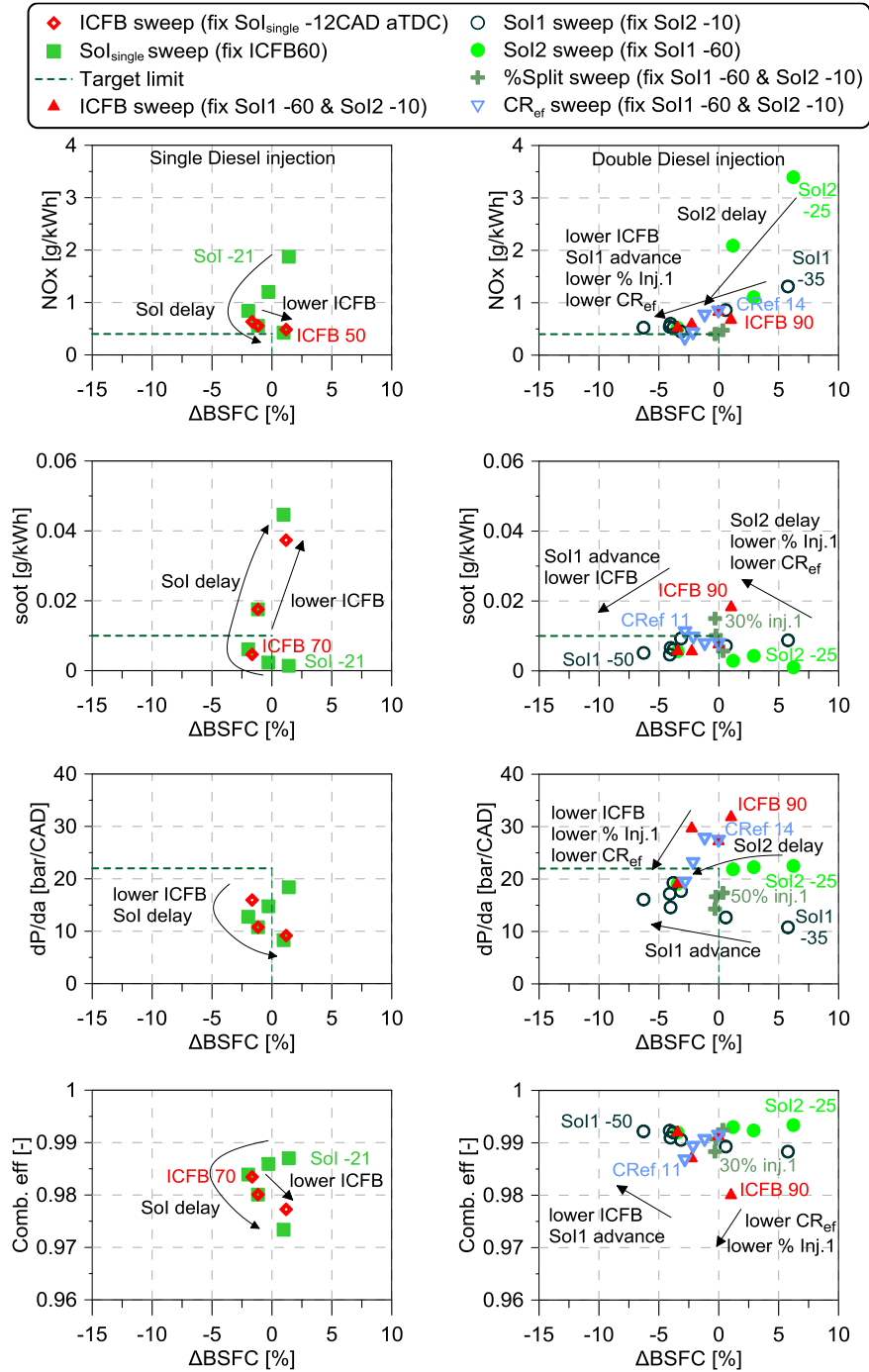
713

Figure 8. Valves strategy employed in realizing the Miller cycle.

714

715

716



717

718

719

Figure 9. Experimental results from the different variables swept at medium load operation, using single Diesel injection (left) and double Diesel injection (right).

720

721

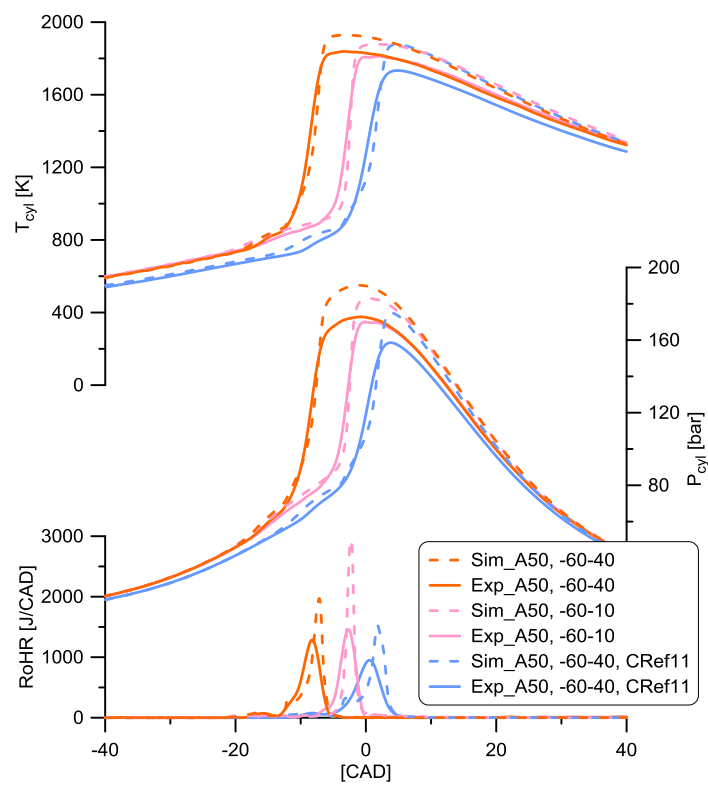
722

723

724

725

726



727

728 Figure 10. RoHR, in-cylinder mean pressure and temperature comparison between
729 modeling and experimental results, for early SoI2 & CR_{ef} 14, late SoI2 & CR_{ef} 14 and
730 early SoI2 & CR_{ef} 11, at ICFB 80 and medium load operation.

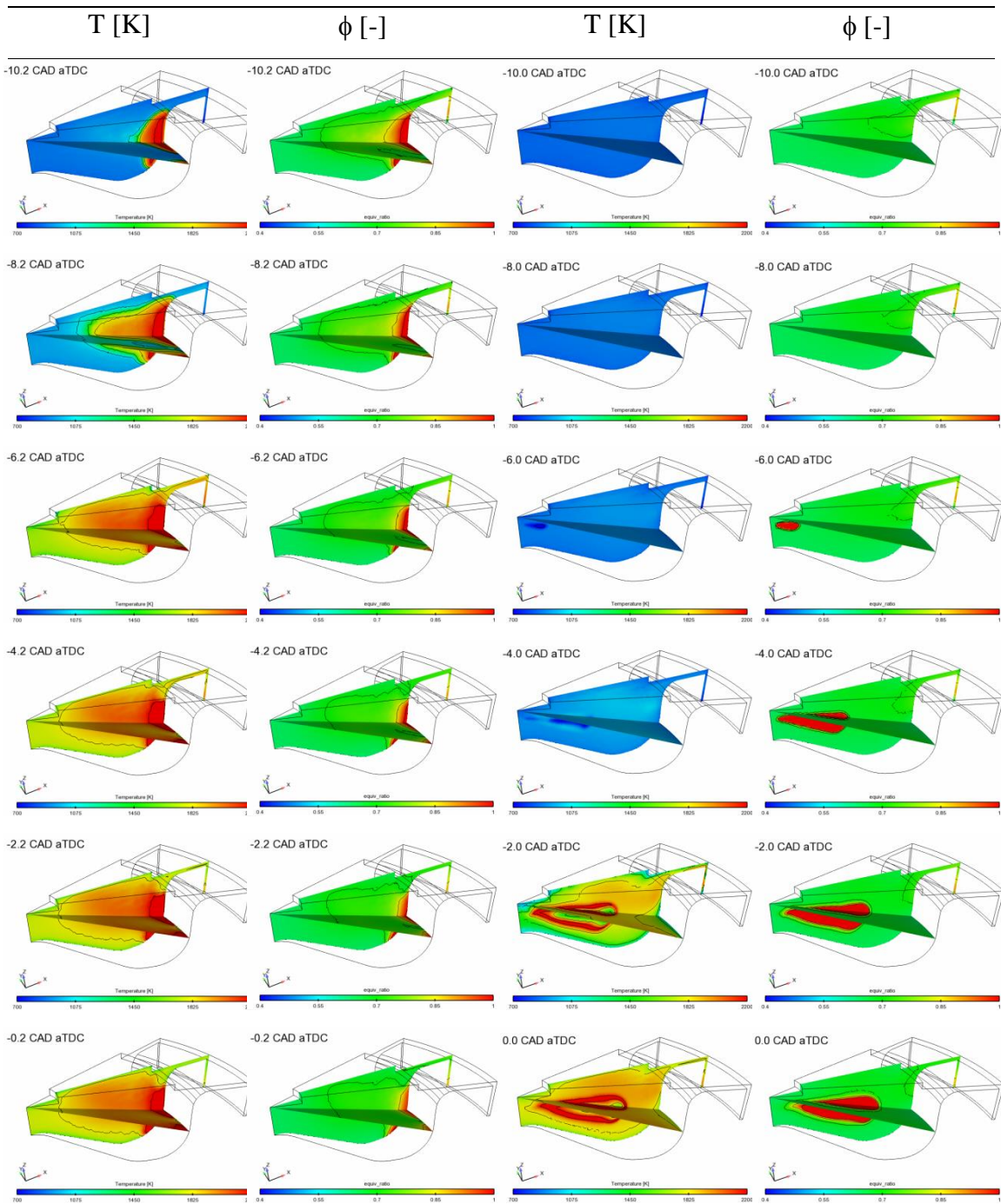
731

732

733

Double + early SoI2 (-60/-40 CAD aTDC)

Double + late SoI2 (-60/-10 CAD aTDC)



734

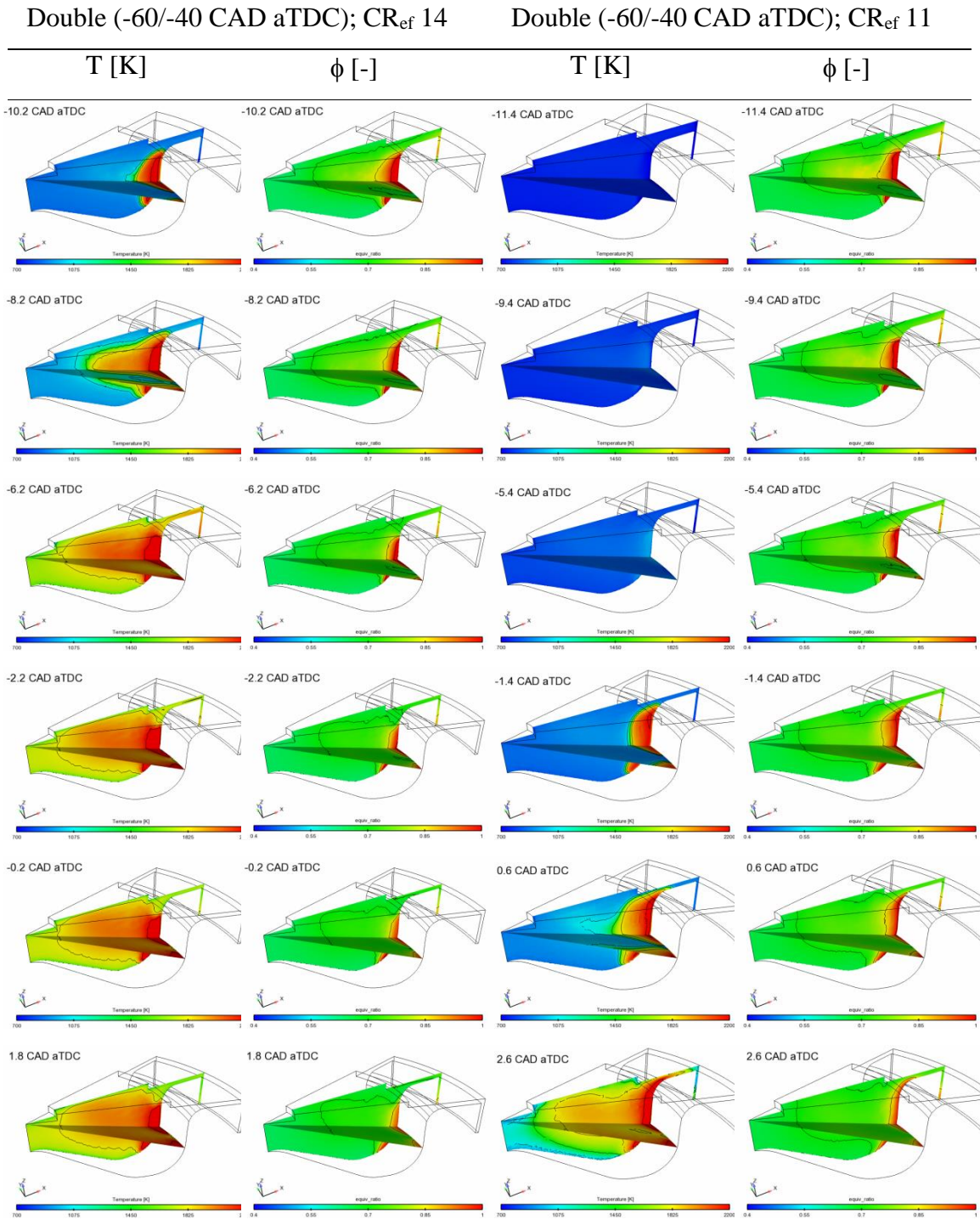
Figure 11. Calculated temperature and equivalence ratio cut planes for medium load,

735

double injection strategies, with early SoI2 (left) and close to TDC SoI2 (right).

736

737

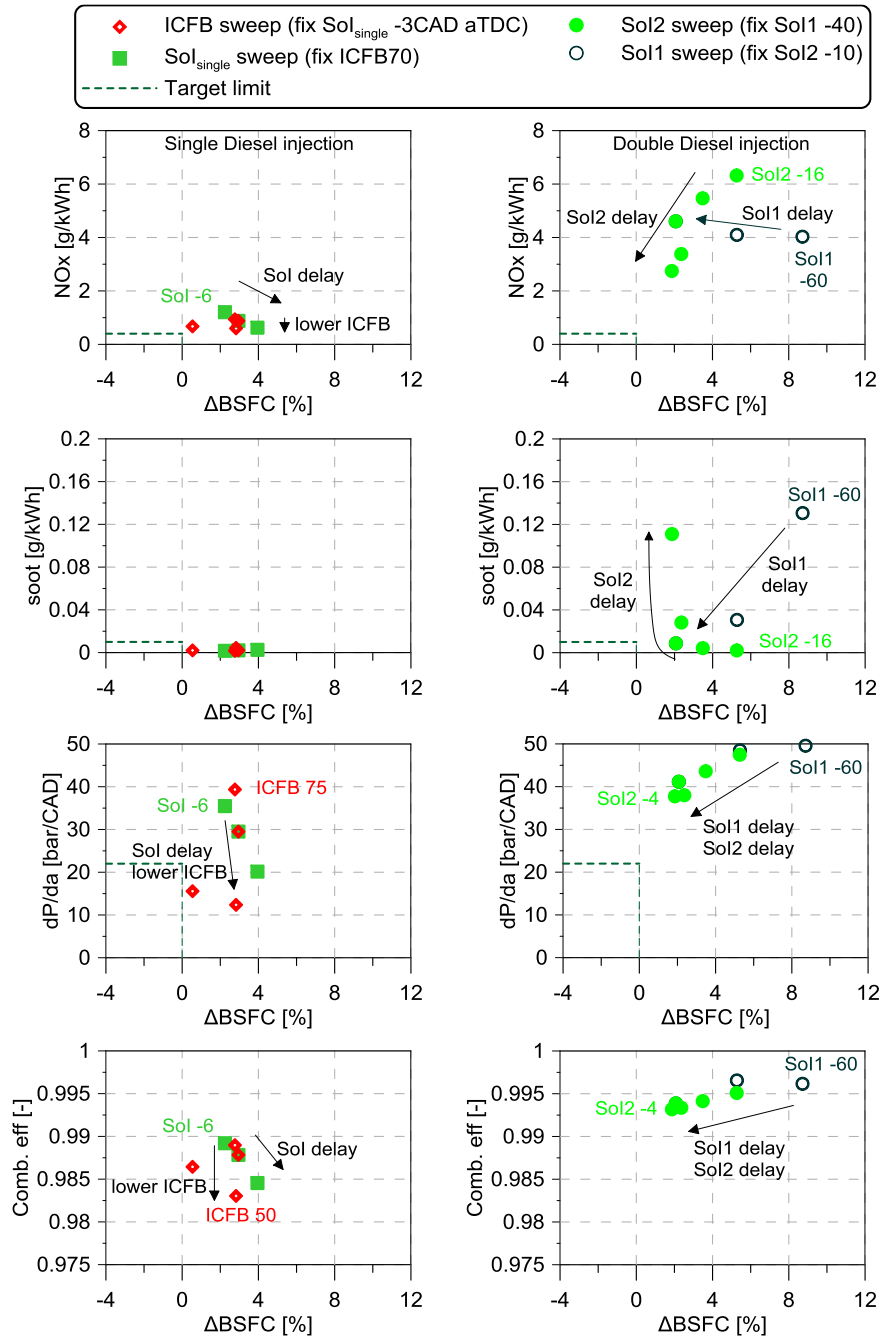


738 Figure 12. Calculated temperature and equivalence ratio cut planes for medium load,
 739 double injection strategies, with CR_{ef} 14 (left) and CR_{ef} 11 (right).

740

741

742



743

744

745

746

Figure 13. Experimental results from the different variables swept at high load operation, using single Diesel injection (left) and double Diesel injection (right).

747

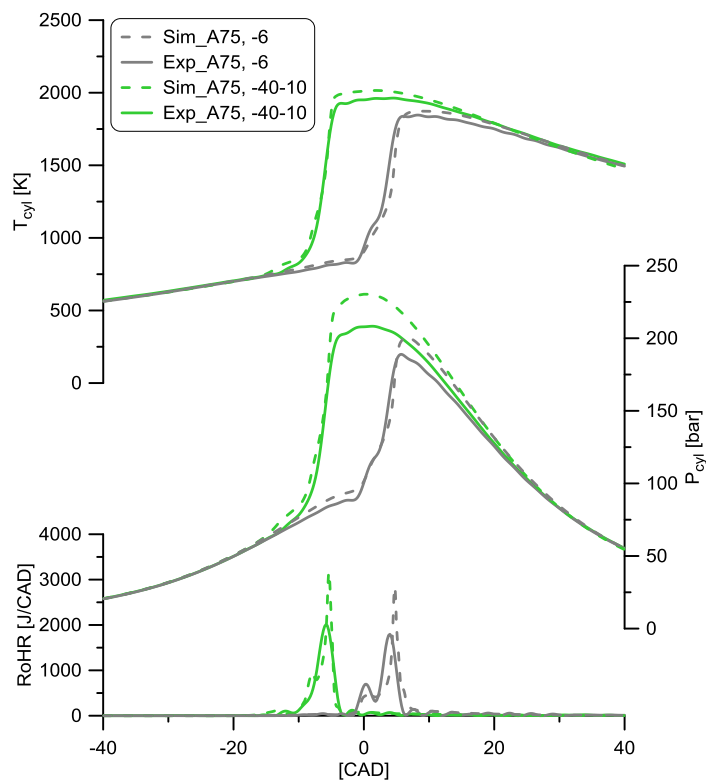
748

749

750

751

752



753

754

755

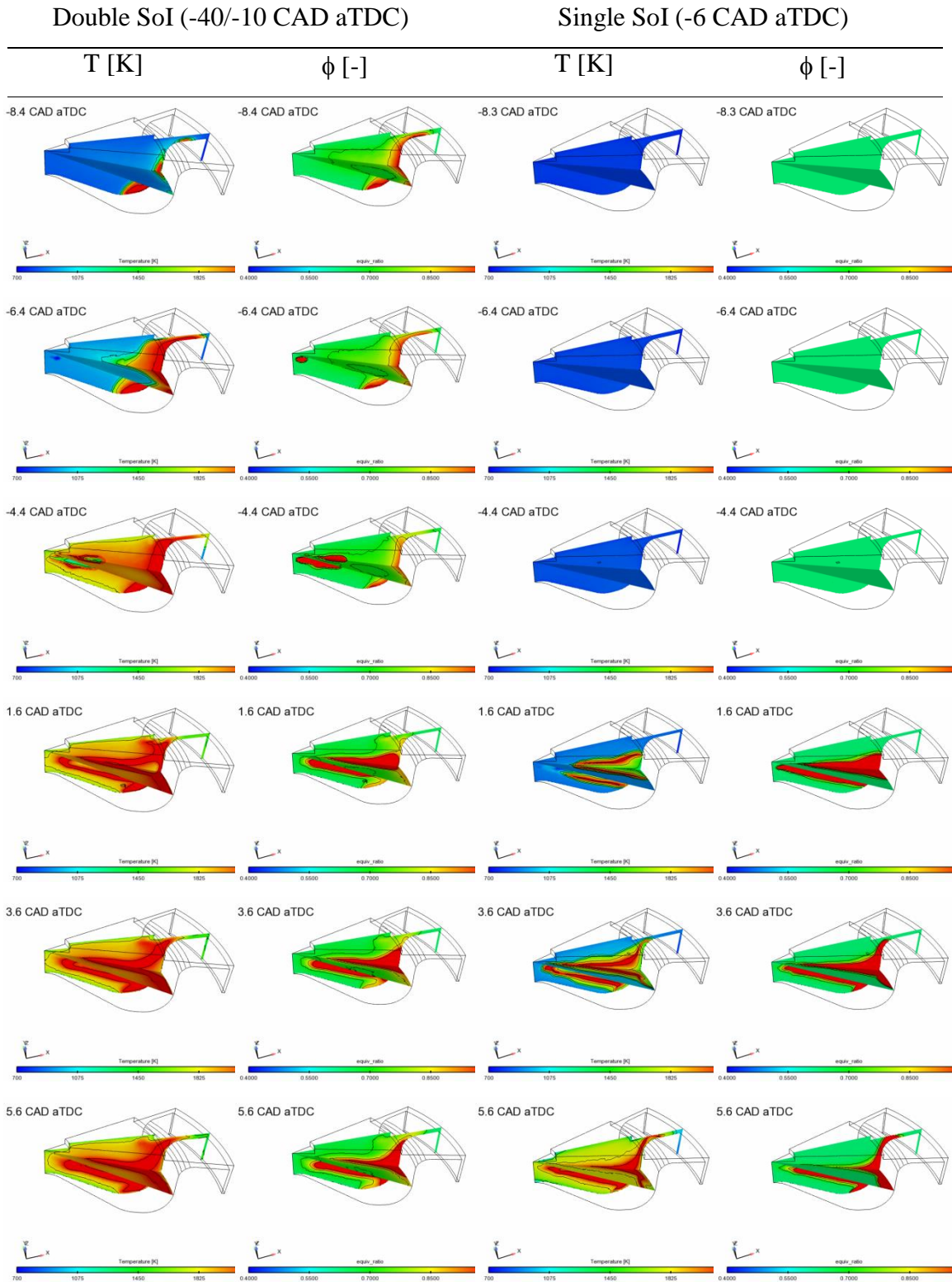
756

Figure 14. RoHR, in-cylinder mean pressure and temperature comparison between modeling and experimental results, for single and double injection strategies, at ICFB 70 and high load operation.

757

758

759



760 Figure 15. Calculated temperature and equivalence ratio cut planes for high load, double
 761 Diesel injection (left) and single Diesel injection (right).
 762

763

764

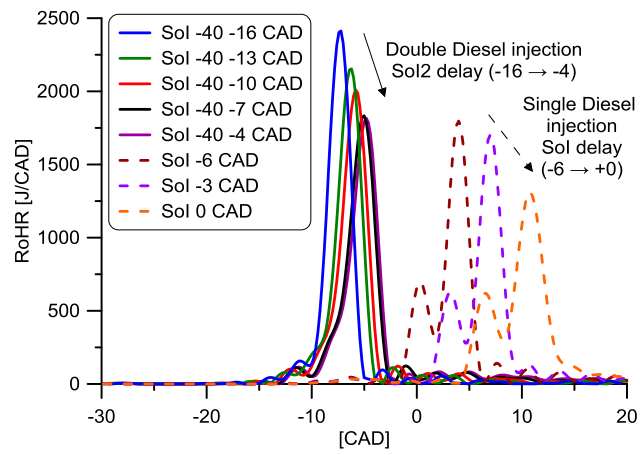
765

766

767

768

769



770

771 Figure 16. RoHR experimental results, from single SoI and SoI2 sweeps, at ICFB 70

772 and high load operation.

773

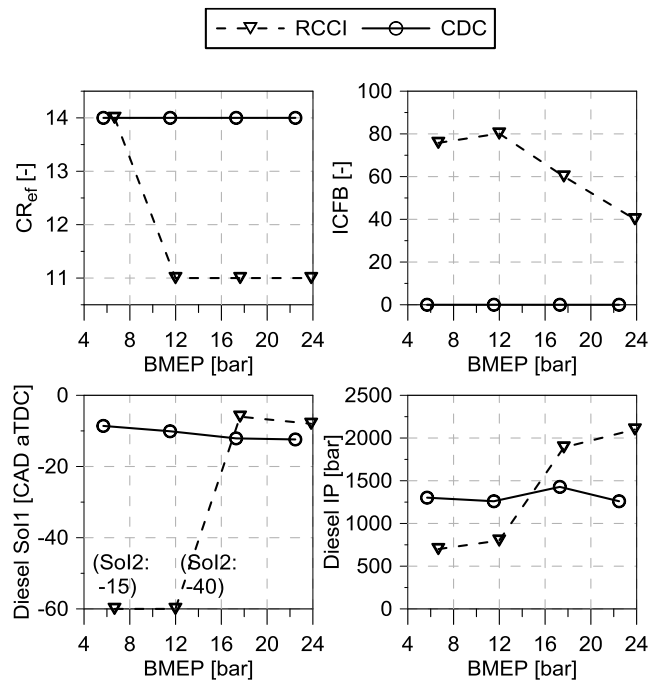
774

775

776

777

778



779

780 Figure 17. Best RCCI settings, selected for full range operation, and CDC settings

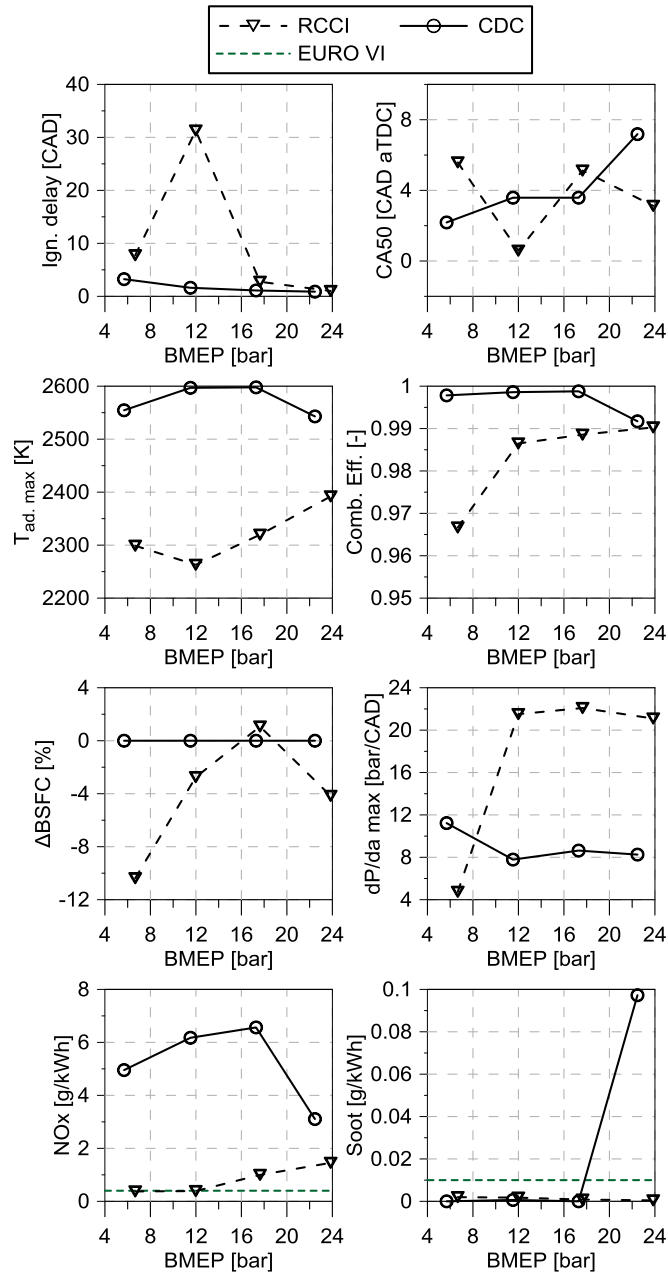
781 provided by the engine manufacturer for analogue operating conditions.

782

783

784

785



786

787 Figure 18. Experimental results from full range RCCI and CDC operation, in terms of
 788 performance and emissions.

789

790

Paper draft:

Operating range extension of RCCI combustion concept from low to full load in a heavy-duty engine

791 **List of Tables**

1. Engine basic specifications	36
2. Fuels main properties	37
3. Detailed conditions, fixed and (swept), for the parametric studies of the low, medium and high load operation, for the RCCI operation range extension.	38

792

793
794
795
796
797
798
799
800
801
802
803
804
805
806
807
808
809

Table 1. Engine basic specifications.

Engine type	Single cylinder, 4 stroke cycle
Bore x stroke [mm]	123 x 152
Connecting rod length [mm]	225
Displacement [cm ³]	1.806
Geometric compression ratio [-]	14.4:1
Number of valves [-]	4
Valve actuation system	Camless HVA
Diesel fuel injection system	Bosch CRSN 4.2 direct injection Common-rail, Amplifier-piston
Diesel injection nozzle	9 holes, 0.168 mm, 142 deg
Gasoline injection system	Low pressure, 2 port fuel injectors
Port fuel injector model	Bosch EV14 KxT

810
811
812
813

Paper draft:

Operating range extension of RCCI combustion concept from low to full load in a heavy-duty engine

814
815
816
817
818
819
820
821
822
823
824
825
826
827
828
829
830

Table 2. Fuels main properties.

		Gasoline	Diesel
Density (T=15°C)	[kg/m³]	735	824
Viscosity (T=40°C)	[cSt]	0.45	2.8
Octane Number	[-]	98	-
Cetane Number	[-]	-	52
Lower Heating Value	[kJ/kg]	43950	42920

831
832
833
834

835
836
837
838
839
840
841
842
843
844
845
846
847
848
849
850
851

Table 3. Detailed conditions, fixed and (swept), for the parametric studies of the low, medium and high load operation, for the RCCI operation range extension.

		(a)	(b)	(c)
		Low load	Medium load	High load
Speed	[rpm]	1200	1200	1200
Air mass flow	[kg/h]	53.3	86	118
Total fuel	[mg/cycle]	70	119	175
ICFB (single inj.)	[%]	75 (65 → 85)	60 (50 → 70)	70 (50 → 75)
Diesel SoI (single inj.)	[CAD aTDC]	-24 (-15 → -24)	-12 (-9 → -21)	-3 (0 → -6)
Diesel IP (single inj.)	[bar]	1000	1175	1890
ICFB (double inj.)	[%]	-	60 (60 → 90)	-
Diesel SoI1 (double inj.)	[CAD aTDC]	-60 (-25 → -60)	-60 (-35 → -65)	-40 (-40 → -60)
Diesel SoI2 (double inj.)	[CAD aTDC]	-15 (-15 → -50)	-10 (-10 → -25)	-10 (-4 → -16)
Diesel ratio (double inj.)	[%SoI1]/[%SoI2]	(40/60 → 60/40)	(30/70 → 50/50)	50/50
Diesel IP (double inj.)	[bar]	700	800	900
CR_{ef}	[-]	14	(14 → 11)	11
P_{int}	[bar]	1.35	(2.2 → 2.92)	3.39
T_{int}	[°C]	40	40	32
YO₂ IVC	[%]	15.5	15.1	16.3

852
853